SPACE-CHARGE EFFECTS IN H⁻ LOW ENERGY BEAM TRANSPORT OF LANSCE

Y.K.Batygin[#], C.Pillai, L.J.Rybarcyk, LANL, Los Alamos, NM 87545, USA

Abstract

The 750-keV low-energy beam transport of the Los Alamos Neutron Science Center (LANSCE) linac consists of two independent beam lines for simultaneous injection of H^+ and H^- beams into the linear accelerator. While transport of the H^+ beam is seriously affected by uncompensated space charge forces, the same effect for H^- is hidden by the presence of multiple beam collimators and beam chopping. Recent results from beam development experiments indicate a significant influence of space charge on H^- beam dynamics in the low-energy beam transport. Measurements of beam emittance along beam transport show the formation of S-shaped filamentation in the particle distribution phase space, typical with the presence of non-linear space charge forces. Results are supported by particle tracking simulations with the PARMILA, BEAMPATH, and TRACE codes.

LANSCE LOW-ENERGY BEAM TRANSPORT

The H beam injector includes a cesiated, multicusp-field, surface –production ion source and two-stage low-energy beam transport line. In the first stage, extracted beam is accelerated up to 80 keV, and then is transported through a solenoid, electrostatic deflector, a 4.5° bending magnet, and a second solenoid. The 670 kV Cockroft-Walton column accelerates beam up to energy of 750 keV. The 750 keV LEBT (see Fig. 1) consists of a quadrupole lattice, 81° and 9° bending magnets, slow-wave chopper, RF bunchers, an electrostatic deflector, diagnostics and steering magnets to prepare beam before injection into Drift Tube Linac (DTL). Slit-collector beam emittance measurements at 750 keV are performed at five locations: 1) TBEM1 (just after the Cockroft -Walton column), TBEM2 (downstream of the chopper), 3) TBEM3 (downstream of the 81° bend before RF pre-buncher), 4) TBEM4 (between the first RF (pre)-buncher and second (main) buncher), and TDEM1 (before the entrance to the DTL).

RESULTS OF MEASUREMENTS

During beam development time in 2010 we performed a series of beam emittance and beam profile scans along 750 keV H- beam transport. The purpose of the measurements was to determine the effect of space charge on beam emittance and the level of space charge neutralization of the beam. Measurements were performed with the beam pulse length of 150 µs, repetition rate of 4 Hz, with sampling taking place at the last 50 µs of the pulse. Measurements were performed with ion source pulse length of 825 μs, while measured beam pulse of 150 μs is taken after first 200 μs of ion source pulse.

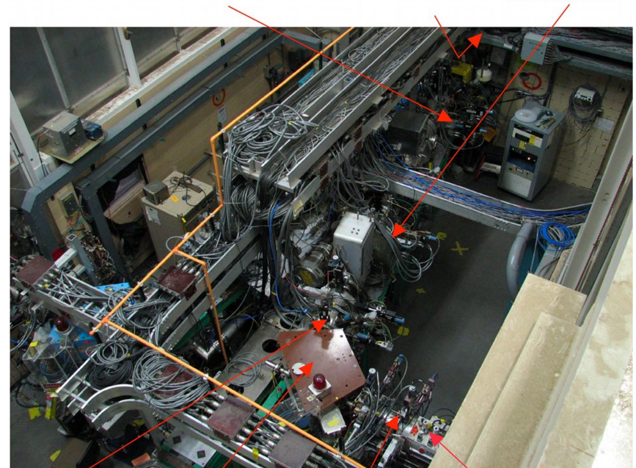

Figure 1. Layout of H^- Low Energy Beam Transport of LANSCE.

Results of measurements were compared with simulation results of TRACE, PARMILA, and BEAMPATH codes. Measured beam distributions at the starting station TBEM1 were reproduced in a macroparticle model as the initial distribution for subsequent beam simulations. Fig. 2 illustrates measured beam emittance data taken at the middle of the transport (station TBEM3) and at the end of the transport (station TDEM1). Measured beam emittance projections exhibit the presence of S-shaped distortions in the distributions. The appearance of S-shaped beam distribution is attributed to the presence of uncompensated space charge forces. For comparison, Fig. 2 contains results of simulated beam transport with zero current and with full current of I = 15 mA. As expected, in case of negligible current, beam does not experience filamentation in phase space.

At each measurement station we compared equivalent beam ellipses obtained from measurement and from simulaton, and calculated the mismatch factor between them [1]

$$F = \sqrt{\frac{1}{2}(R+\sqrt{R^2-4})} - 1 \qquad (1)$$

where $R = \beta_{exp}\gamma_s + \beta_s\gamma_{exp} - 2\alpha_{exp}\alpha_s$ is the parameter indicating overlapping of beam ellipses with Twiss parameters obtained from experiment, α_{exp}, β_{exp}, γ_{exp}, and from simulations α_s, β_s, γ_s. Table 1 contains results

[#]batygin@lanl.gov

of a comparison of beam dynamics with and without space charge forces. The mismatch factor is significantly smaller for simulations runs with full current of I = 15 mA. From that we conclude that the beam transport is space-charge uncompensated.

An additional set of measurements were performed for comparison of measured and simulated Twiss parameters between TBEM3 and TBEM4 stations allowing beam propagation in the drift space between stations. The measured Twiss parameters and beam emittances at TBEM3 served as initial data for beam tracking. Resultant values at the end of simulation distance were compared with measured data at TBEM4. The value of beam current was adjusted to get the final data as close as possible to the measured data at the final point of tracking. Fig. 3 illustrates the value of mismatch factor F for indication of beam deviation from the desired values as a function of beam current for beam tracking between TBEM3 and TBEM4. The mismatching factor has a minimum around I = 20 mA which is close to nominal value of beam current of 15 mA used in experiment.

Another set of simulations was performed with initial equivalent elliptical distributions (Water Bag, Parabolic, Gaussian) with the same rms parameters as that of measured distribution at initial station TBEM1. Results of simulations show that while elliptical models demonstrate qualitatively similar filamentation in phase space, they do not exhibit the same level of filamentation as that with actual distribution. Therefore, simulations with particle distributions taken directly from experiment are essential for realistic reproduction of beam dynamics.

SPACE CHARGE ABERRATION

To give an analytical treatment of the process of filamentaion in phase space, we consider a redistribution of the Gaussian beam under self space charge forces. The space charge density and space charge field of the beam with Gaussian distribution are:

$$\rho(r_o) = \frac{2I}{\pi R_o^2 \beta c} \exp(-2\frac{r_o^2}{R_o^2}), \quad (2)$$

$$E_b = \frac{I}{2\pi \varepsilon_o \beta c} \frac{1}{r_o} [1 - \exp(-2\frac{r_o^2}{R_o^2})], \quad (3)$$

where I the beam current, R_o is the beam radius, and β is the beam velocity. Nonlinear space charge field function is expanded as

$$f(r_o) = 1 - \exp(-2\frac{r_o^2}{R_o^2}) \approx 2\frac{r_o^2}{R_o^2} - 2\frac{r_o^4}{R_o^4} + \dots \quad (4)$$

At the initial stage of beam transport, we can assume, that particle radius is unchanged, while the slope of the trajectory is changed. It gives us the nonlinear transformation:

$$r = r_o, \qquad r' = r_o' + \frac{2zP^2}{R_o^2} r_o - \frac{2zP^2}{R_o^4} r_o^3, \quad (5)$$

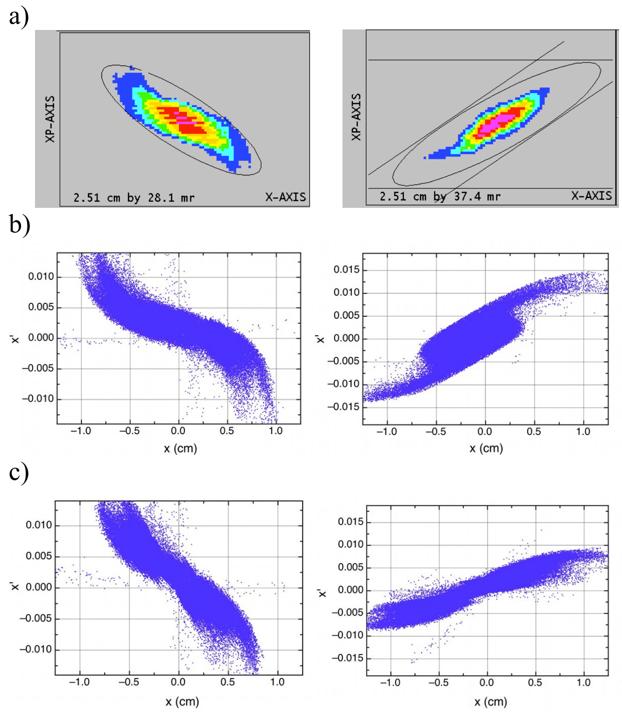

Figure 2: Comparison of measured and simulation results at (left) TBEM3 and (right) TDEM1 beam emittance stations: (a) measurements, (b) simulation with current I = 15 mA, (c) simulation with current I = 0.

Table 1. Mismatch factor F between emittance measurements and simulations.

	BEAMPATH		TRACE	
Station	$I = 0$	I = 15mA	$I = 0$	I = 15mA
TBEM1	0	0	0	0
TBEM2	0.22	0.20	0.626	0.359
TBEM3	0.24	0.175	0.648	0.513
TBEM4	0.39	0.23	0.935	0.428
TDEM1	0.41	0.15	1.161	0.565

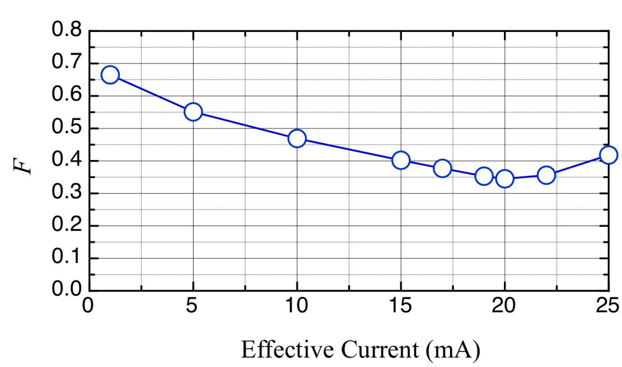

Figure 3. TRACE mismatch factor F as a function of beam current in beam drift between TBEM3 and TBEM4.

where $P^2 = 2I/(I_c \beta^3 \gamma^3)$ is the generalized perveance. Suppose, initial beam distribution is bounded by an ellipse:

$$\frac{x_o^2}{R^2}\varepsilon + \frac{x_o'^2}{\varepsilon} R^2 = \varepsilon, \quad (6)$$

where ε is the beam emittance. Substitution of transformation, Eqs. (5), into the ellipse equation (6), and changing variables (x, x') to action-angle variables (J, ψ) gives us the beam ellipse distortion:

$$T + T^2 2\upsilon \sin\psi \cos^3\psi + T^3\upsilon^2 \cos^6\psi = 1 , \qquad (7)$$

where $$T = \frac{2J}{\varepsilon}, \qquad \upsilon = \frac{2zP^2}{\varepsilon} . \qquad (8)$$

Equation (7) describes the boundary of the new phase space volume, occupied by the beam (see Fig. 4). Without the nonlinear perturbation, $\upsilon = 0$, equation (7) describes an ellipse (circle) in phase space. If $\upsilon \neq 0$, equation (7) describes the S - shape figure of beam emittance.

BEAM PERFORMANCE UNDER DIFFERENT VACUUM CONDITIONS

Additional beam emittance and profile measurements were performed along LEBT under different vacuum conditions. To manipulate the vacuum conditions, we had to override pump and valve interlocks to maintain beam run permit and to allow manual throttling of the vacuum valves.

During the measurements, we observed a significant reduction of beam current along transport with worsening vacuum conditions (see Fig. 5), while the beam emittance remained approximately the same (see Fig. 6). One possible explanation is related to H^- beam stripping under degraded vacuum conditions. One can estimate a value of the H^- stripping cross section from the measurements,

$$\sigma = \left(\frac{\Delta I}{I}\right)\frac{1}{nl} = 3\cdot 10^{-16}\, cm^2 \qquad (9)$$

where $\Delta I/I$ is the observable beam losses, n is the residual gas density, and l is the transport length. This estimate coincides well with published data on cross section of stripping of H^- beam in N_2 and O_2 residual gases [2]. The observation that the beam emittance does not grow is consistent with estimates of multiple elastic scattering to be small for this case. An additional observation was the reduction of beam current in LEBT resulted in smaller beam sizes and better beam emittance at the end of the linac.

SUMMARY

A study of 750 keV H^- beam transport was performed. The beam experiences phase-space distortions, S-shaping, typical for space charge aberrations. Analysis of mismatch factor comparing measured and simulated distributions, together with observed distortion of phase space of the beam, support the conclusion that H^- beam transport is space-charge uncompensated.

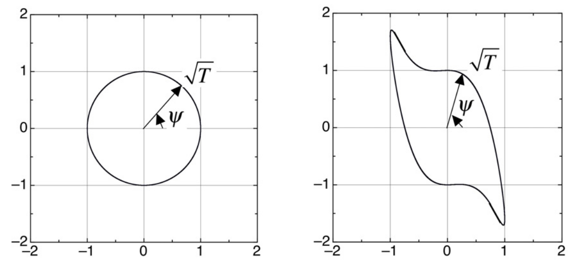

Figure 4. Distortion of beam emittance due to aberrations, Eq. (7): (left) nonlinear perturbation $\upsilon = 0$, (right) $\upsilon = 1.6$.

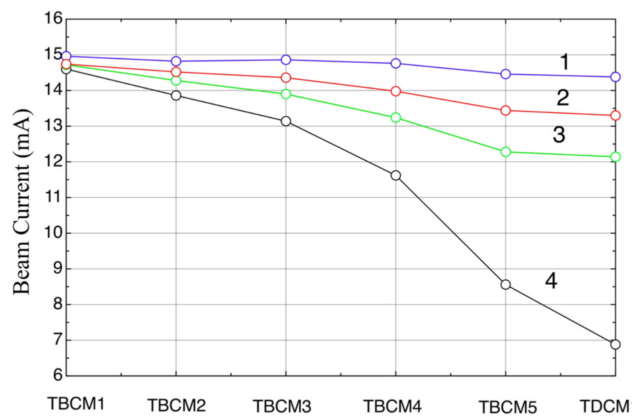

Figure 5. Beam transmission through LEBT as a function of vacuum conditions: (1) $4.6\cdot 10^{-7}$ Torr, (2) $7.4\cdot 10^{-6}$ Torr, (3) $1.3\cdot 10^{-5}$ Torr, (4) $4.9\cdot 10^{-5}$ Torr.

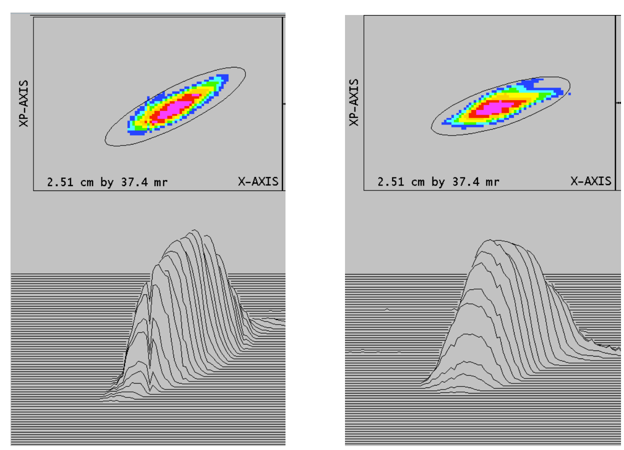

Figure 6. TDEM1 emittance scan with (left) nominal vacuum of $7\cdot 10^{-7}$ Torr and (right) with vacuum of $3\cdot 10^{-5}$ Torr.

REFERENCES

[1] K.R.Crandall and D.P.Rusthoi, TRACE 3-D Documentation, LA-UR-97-886 (1997).
[2]. Atomic Data for Controlled Fusion Research, ORNL-5206 (1977).